RESEARCH ARTICLE

The effect of water stress on net primary productivity in northwest China

Zhenyu Zhang [1,2,3] · Weimin Ju [1] · Yanlian Zhou [2]

Abstract

Net primary productivity (NPP) has been widely used as the indicator of vegetation function and exhibits large spatial and temporal variations caused by numerous factors. Northwest China (NWC) is one of the driest regions in China, and water supply is the key determinant of NPP here. However, studies on the effects of water stress on NPP in NWC at the regional scale are still relatively lacking. Thus, in this study, based on a set of Moderate-Resolution Imaging Spectroradiometer (MODIS) NPP and evapotranspiration (ET) datasets, we quantified the response of NPP to water stress, which is indicated by crop water stress index (CWSI). Regional average of annual NPP in NWC showed an increasing trend during the study period, at a rate of 0.84 g C m^{-2} yr^{-1}. At the province level, the NPP increase rates increased in the order of Ningxia (7.7%), Shaanxi (6.5%), Gansu (4.5%), Qinghai (3.8%), and Xinjiang (1.7%). NPP was negatively correlated with CWSI ($p<0.05$) in 73% of areas, indicating the key role of water stress in constraining NPP over this arid region. The effect of water stress on NPP changes with elevation. Water stress has the strongest negative impact on NPP in areas with elevations around 2000 m. In elevations above 5000 m, NPP is not limited by water stress, mostly positively correlated with CWSI. Our findings further clarify the importance of water stress in dryland ecosystems, while highlighting that elevation gradients can significantly affect the correlation between NPP and water stress.

Keywords Net primary productivity · Crop water stress index · Water stress · Elevation gradient · Arid region · Northwest China

Introduction

As a key component of the terrestrial carbon cycle, net primary productivity (NPP) refers to the difference between organic matter fixed through photosynthesis and accumulated respiration consumption per unit area and per unit time of green plants (Cramer and Field 1999; Euskirchen et al. 2002). NPP is an effective and important indicator of vegetation functioning and health. It is a key determinant of terrestrial carbon

✉ Weimin Ju
juweimin@nju.edu.cn

[1] International Institute of Earth System Science, Nanjing University, Nanjing 210023, China

[2] School of Geography and Ocean Science, Nanjing University, Nanjing 210023, China

[3] State Key Laboratory of Subtropical Silviculture, Zhejiang A&F University, Zhejiang 311300, Hangzhou, China

sinks and sources, which play an important role in retarding the rate of atmospheric CO_2 increase and global warming. NPP data are useful in many applications and increasingly relevant to decision-making. Owing to influences of climate, soils, land cover types, and human activities, NPP has considerable spatial and temporal variations.

Previous studies have examined the effects of water stress on NPP from the perspective of various meteorological factors, such as temperature (Ciais et al. 2005; Nemani et al. 2003), precipitation (Zhang et al. 2020a), and atmospheric vapor pressure deficit (Feng et al. 2007; Saigusa et al. 2008). In general, extreme heat and reduced precipitation will induce sharp reduction of NPP (Penuelas et al. 2007; Tatarinov et al. 2016). Meanwhile, increased atmospheric vapor pressure deficit also inhibits NPP (Penuelas et al. 2007, Tatarinov et al. 2016). However, water stress is an integrated effect that should be more closely linked to the vegetation (Hsiao 1973; Munns 2002). The analysis on the relationship between single meteorological factor and NPP is unable to consider the integrated influence of other factors on NPP (Hein et al. 2019; Liu et al. 2020). Therefore, an indicator that integrates multiple

meteorological factors is required for better indicating the impact of water stress on the NPP.

Crop water stress index (CWSI) (Jackson et al. 1981), which combines multiple meteorological factors, has been widely used in agricultural drought monitoring (Berni et al. 2009; Pou et al. 2014), owing to its ability to capture water stress caused by increased temperature or/and decreased precipitation and its close linkage with vegetation growth (Irmak et al. 2000). Kullberg et al. (2017) compared multiple drought indices and found that CWSI was more sensitive to small changes in water stress. Gerhards et al. (2016) analyzed the relationship between CWSI and potato growth status and found a high agreement between them. Na et al. (2020) also found a high agreement between CWSI and cabbage growth status. Thus, CWSI could be an effective indicator for analyzing the influence of water stress on NPP.

Northwest China (NWC) is one of the most ecologically fragile regions in China and has received a great deal of research attention (Li et al. 2020; Yao et al. 2020). Though many studies have indicated that vegetation growth is seriously limited by water supply in NWC (Pan et al. 2020; Zhang et al. 2020b), quantitative research on the effect of water stress on vegetation growth at the landscape scale is still lacking.

With MODIS NPP, evapotranspiration (ET), and potential evapotranspiration (PET) datasets, this study is to answer the above question. The specific objectives of this study are (1) to investigate spatial and temporal variations of NPP in NWC; (2) to quantitatively analyze changes of water stress indicated by CWSI in NWC; and (3) to quantitatively assess the response of NPP to water stress in recent years in NWC.

Materials and methods

Study area

NWC (73°15′ E–111°15′ E, 31°32′ N–49°10′ N) occupies one-third of China's area and includes five provinces and autonomous regions (Fig. 1), namely Shaanxi, Qinghai, Gansu, Ningxia, and Xinjiang. Plateau, basin, and mountainous areas are the main terrains in this region. Most areas have temperate continental climate and high cold climate (Gong et al. 2018). Annual precipitation decreases from 400 mm a^{-1} in the eastern region to 200 mm a^{-1} in the western region, even below 50 mm a^{-1}. The harsh natural condition causes low NPP with significant variability here (Wang et al. 2019).

Materials

Net primary productivity dataset

Monthly MODIS NPP (http://files.ntsg.umt.edu/data) at a spatial resolution of 1km ×1km over the period from 2000
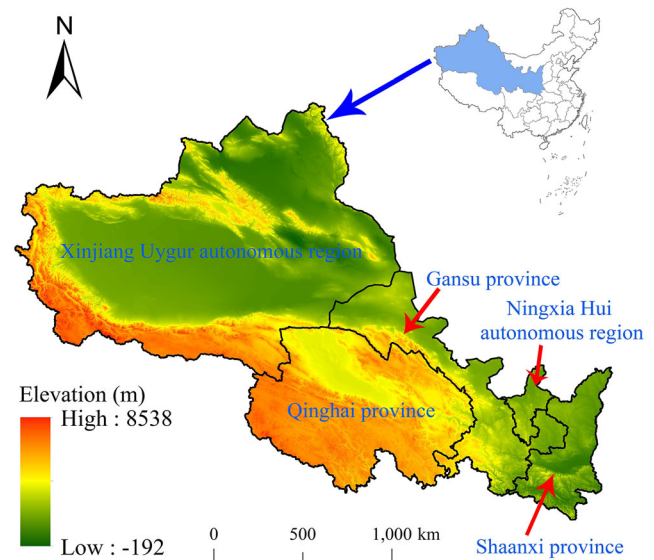

Fig. 1 Location of NWC

to 2015 was used in this study. It is produced using the MOD17A3 algorithm (Running et al. 2004). MODIS NPP is calculated as the residual of gross primary productivity (GPP) minus autotrophic respiration. GPP is calculated using a light use efficiency model, and autotrophic respiration is estimated according to temperature and biomass approximated by remotely sensed vegetation parameters (Fensholt et al. 2006; Zhao et al. 2005). MODIS NPP data has been used in studies on vegetation changes at different scales (Azhdari et al. 2020; Bastos et al. 2013; Hasenauer et al. 2012; Li et al. 2019; Street and McNickle 2019; Turner et al. 2006; Wang et al. 2020b).

Evapotranspiration (ET) and potential evapotranspiration (PET) dataset

Monthly MODIS ET and PET data (MOD16A3) (Nagler et al. 2005; Velpuri et al. 2013; Yuan et al. 2010) at a spatial resolution of 0.05 × 0.05 over the period from 2000 to 2014 were used for calculating CSWI. They were available at https://modis.gsfc.nasa.gov/. MODIS ET and PET data are calculated using the Penman-Monteith equation (Monteith 1965, 1981). Detailed information regarding to the calculation of ET and PET can be found in Mu et al. (2011).

MODIS ET and PET were resampled into a spatial resolution of 1km with a projection of WGS_1984_UTM_Zone_50N using the bilinear interpolation method (Liu and Weng 2018) for better analysis with NPP at pixel level.

Auxiliary data

An elevation data with a spatial resolution of 30 m was acquired from the Shuttle Radar Topography Mission Digital Elevation Model (SRTM DEM) dataset. SRTM DEM dataset

could be downloaded from the Geospatial Data Cloud (http://www.gscloud.cn).

Vegetation cover data was obtained from the Moderate Resolution Imaging Spectroradiometer (MODIS) land cover dataset (MCD12C1). The spatial resolution of MCD12C1 is 0.05°. MCD12C1 could be downloaded from the USGS Earth Explorer (https://earthexplorer.usgs.gov/).

Methods

Change rate and inter-annual variability of NPP

In this study, change rate (Wang et al. 2016b) was used to characterize the dynamics of NPP over the past years. Coefficient of variation (CV), as a statistic indicator representing the degree of variation of a variable, i.e., the ratio of the standard deviation to the mean, was applied to quantify the inter-annual variability of NPP. The two indicators could be calculated as (Alharbi et al. 2019; Rojo Baio et al. 2019):

$$C = \frac{n\sum_{i=1}^{n}(i \times N_i) - \sum_{i=1}^{n}i\sum_{i=1}^{n}N_i}{\overline{N} \times \left[n \times \sum_{i=1}^{n}i^2 - \left(\sum_{i=1}^{n}i\right)^2\right]} \times n \times 100\% \quad (1)$$

$$CV = \frac{1}{\overline{N}}\sqrt{\frac{\sum_{i=1}^{n}\left(N_i - \overline{N}\right)^2}{n-1}} \quad (2)$$

where C is the change rate of NPP N (%); N_i is the value of NPP in time location i in the range from 1 to n; $\overline{N}$ is the average of NPP during the study period; and CV is the coefficient of variation. The larger the CV value, the greater the inter-annual variability of NPP over time.

Mann-Kendall trend and mutation test

Mann-Kendall trend and mutation test were applied to further analyze the trend and mutation status of NPP in individual provinces within NWC. The specific analysis process is as follows:

For a NPP time series data N, the Mann-Kendall trend test statistic variable S is defined as (Burn and Elnur 2002):

$$S = \sum_{p=1}^{m-1}\sum_{q=p+1}^{m}\mathrm{Sgn}(N_q\text{-}N_p) \quad (3)$$

where m is the length of N and N_p and N_q are the pth and qth values of N, respectively. Sgn () is a symbolic function, which is defined as:

$$\mathrm{Sgn}(N_q\text{-}N_p) = \begin{cases} +1 & N_q\text{-}N_p > 0 \\ 0 & N_q\text{-}N_p = 0 \\ -1 & N_q\text{-}N_p < 0 \end{cases} \quad (4)$$

when $n > 10$; the trend significance statistic Z is calculated as:

$$Z = \begin{cases} \dfrac{S\text{-}1}{\sqrt{\mathrm{var}(S)}} & S > 0 \\ 0 & S = 0 \\ \dfrac{S+1}{\sqrt{\mathrm{var}(S)}} & S < 0 \end{cases} \quad (5)$$

$$\mathrm{var}(S) = n(n\text{-}1)(2n\text{-}15)/18 \quad (6)$$

where $\mathrm{var}(S)$ is the variance of S. A positive or negative value of Z indicates an upward or downward trend of N. When $|Z|$ is greater than or equal to 1.96, the trend is significant at the level of 95%.

The Mann-Kendall mutation test method was used to identify the year when the NPP change is abnormal, that is, the year with NPP significantly inconsistent with the past overall NPP change trend. Firstly, we need to construct an order sequence S_k (Rahman et al. 2017):

$$S_k = \sum_{d=1}^{k}\sum_{e}^{d\text{-}1}\alpha_{de} \quad (1 < k \le m) \quad (7)$$

where α_{de} is the discriminant function and k is the length of the selected time series data.

In Eq. (7), α_{de} is calculated as:

$$\alpha_{de} = \begin{cases} 1 & N_d > N_e \\ 0 & N_d < N_e \end{cases} \quad (1 \le e \le d) \quad (8)$$

where N_d and N_e are the dth and eth values of time series data N, respectively.

Secondly, based on S_k calculated using Eq. (7), the first mutation detection variable U_f can be calculated as (Pettitt 1979):

$$U_f = \frac{[S_k\text{-}E(S_k)]}{\sqrt{\mathrm{var}(S_k)}} \quad (9)$$

where $E(S_k)$ and $\mathrm{var}(S_k)$ are the average and variance of S_k, respectively. They are calculated as:

$$E(S_k) = k(k+1)/4 \quad (10)$$

$$\mathrm{var}(S_k) = k(k\text{-}1)(2k+5)/72 \quad (11)$$

After calculating U_f, we need to arrange the time series data X in reverse order and calculate the second mutation detection statistic (recorded as U_b) using Eqs. (6) to (10). Then, we need to plot the test statistic U_f and U_b as line graphs, respectively. If there is an intersection between U_f and U_b, then the

corresponding time of the intersection is the beginning of the NPP mutation (Lou et al. 2017; Xing et al. 2017).

Correlation analysis

In this study, the correlation coefficient between NPP and CWSI was used to indicate the response of NPP to water stress. It was calculated as (Zhang et al. 2007b):

$$r = \frac{\sum_i^n \left(N_i - \overline{N}\right)\left(Q_i - \overline{Q}\right)}{\sqrt{\sum_i^n \left(N_i - \overline{N}\right)^2 \sum_i^n \left(Q_i - \overline{Q}\right)^2}} \tag{12}$$

where r is the correlation coefficient between NPP N and CWSI Q; Q_i is the CWSI value in year i; and $\overline{Q}$ is the multi-year average of CWSI.

CWSI

CWSI indicates the degree that water demand is satisfied. It is calculated as (Drechsler et al. 2019; Ezenne et al. 2019; Jackson 1982):

$$CWSI = 1 - \frac{ET}{PET} \tag{13}$$

where ET and PET are the annual evapotranspiration and annual potential evapotranspiration, respectively. A CWSI value of 0 indicates that evaporative demand is fully satisfied and there is no water stress. A CWSI value of 1 means that ET is zero and serious water stress occurs.

Hurst index

Hurst index is an effective method in time series data prediction, especially in non-stationary time series forecasting (Jiang et al. 2017; Tong et al. 2018; Wu et al. 2017; Xue et al. 2015). In NPP-related studies, Hurst index is also widely used (Li et al. 2021; Liu et al. 2017). Hurst index is flexible for the length of time series, usually more than 10 years (Jia et al. 2020; Qu et al. 2020). In this study, Hurst index (Hurst 1951) was used to determine whether the future trend of NPP is consistent with the past. It is calculated as:

(1) Given a NPP time series N_i, $i = 1, 2, ... n$, mean series $MEAN_\tau$ with different lengths of time τ ($1 \leq \tau \leq n$) are constructed as:

$$MEAN_\tau = \frac{1}{\tau} \sum_i^\tau N_i \tag{14}$$

(2) The cumulative deviation (CD), extreme deviation (ED), and standard deviation (SD) and process parameter G are calculated as:

$$CD(i, \tau) = \sum_{u=1}^i (N_u - MEAN_\tau) \tag{15}$$

$$ED(i, \tau) = \max CD(i, \tau) - \min(i, \tau) \tag{16}$$

$$SD(\tau) = \left[\frac{1}{\tau} \sum_{i=1}^\tau (N_i - MEAN_\tau)^2\right]^{0.5} \tag{17}$$

$$G(\tau) = \lg \frac{ED(i, \tau)}{SD(\tau)} \tag{18}$$

(3) The linear relationship between $G(\tau)$ and $\lg(\tau)$ is fitted using the least square method (Cox and Matuschak 1941), and the slope obtained is the Hurst index.

Hurst index ranges from 0 to 1 and was used to determine the consistency of future NPP trend with that in the past. When Hurst index is between 0 and 0.5, the future trend of NPP is contrast to the past (this trend is unsustainable) (Pan and Dong 2018). When Hurst index is 0.5, it means the future trend of NPP has no connection to the past. When the Hurst index is between 0.5 and 1, it means the future trend of NPP is consistent with the past (this trend is sustainable) (Li and Pan 2018).

Results

Spatial patterns of NPP in NWC

Figure 2a shows the distribution pattern of multi-year mean annual NPP in NWC. There is distinguishable heterogeneity of NPP in NWC. Overall, NPP decreases gradually from east to west. NPP in the southeastern region was usually above 400 g C m^{-2} yr^{-1}. At the provincial level (Fig. 2b), Shaanxi has the highest NPP with a multi-year average value of 347.92 g C m^{-2}, followed by Gansu (316.53 g C m^{-2}), Ningxia (173.38 g C m^{-2}), Xinjiang (145.4 g C m^{-2}), and Qinghai (118.31 g C m^{-2}).

Figure 2c shows the CV spatial distribution of annual NPP in NWC. NPP exhibited strong inter-annual variability in north-central Shaanxi, southern Ningxia, western Qinghai, and the Kunlun Mountains in western Xinjiang with CV values above 0.2. Averaged over the entire study area, CV was equal to 0.156. As to each province (Fig. 2d), NPP had the largest inter-annual variability in Ningxia with an average CV value of 0.188, followed by Shaanxi, Qinghai, and Xinjiang with average CV values of 0.168, 0.161, and 0.154, respectively. Gansu had the smallest average CV value of 0.134. Overall, the provincial average CV decreased with the increase of annual NPP.

Temporal changes of NPP in NWC

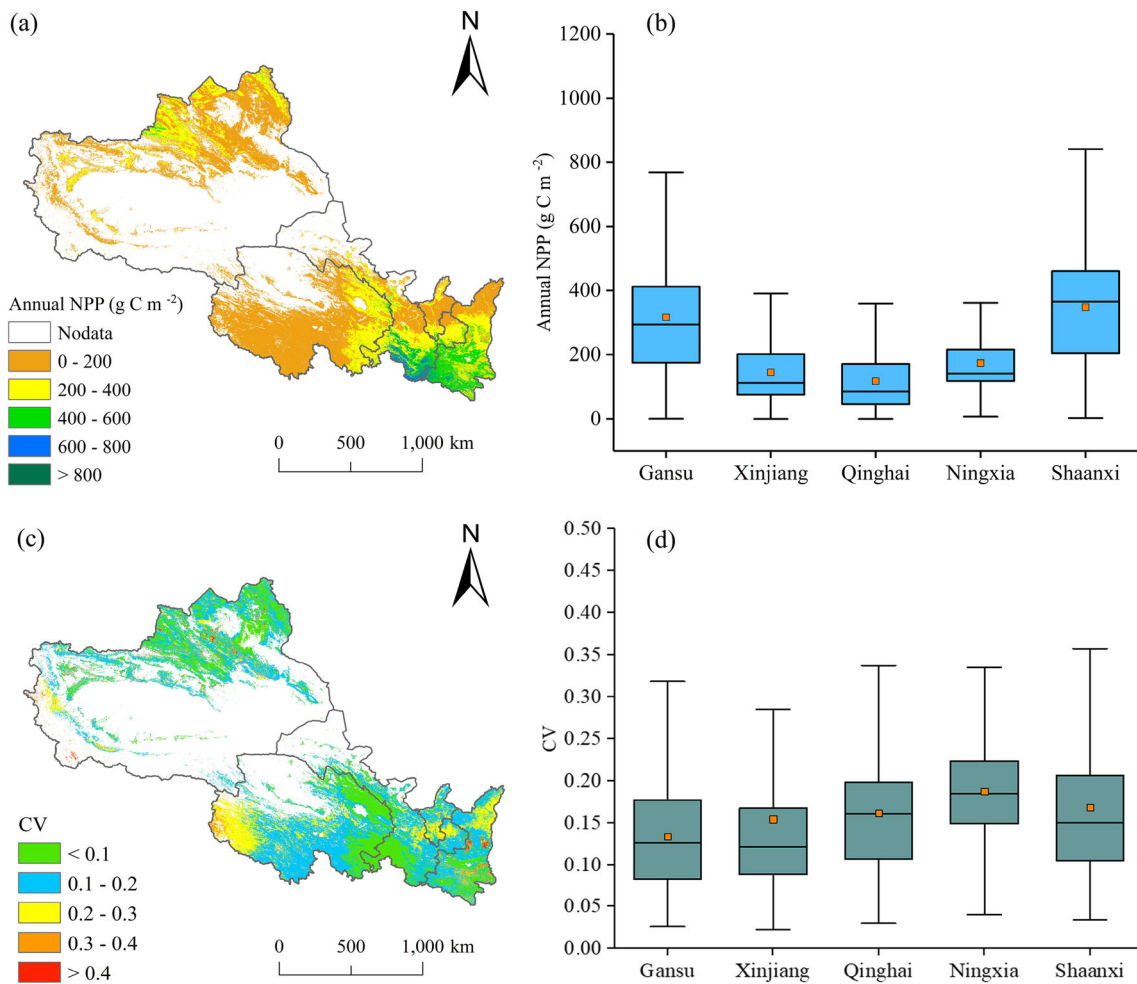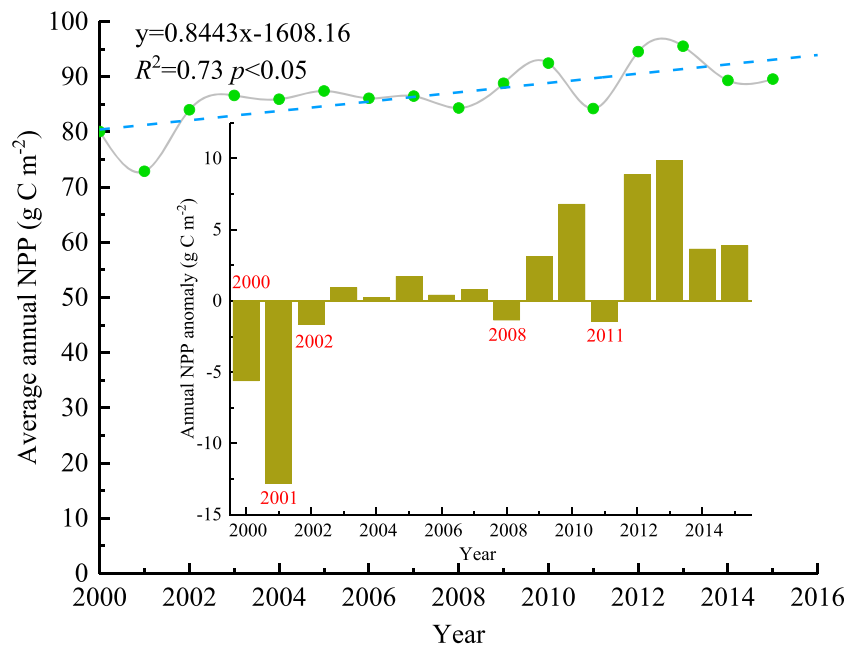Figure 3 shows the change trend of regional average annual NPP and its anomalies during 2000 to 2015 in NWC. NPP

Fig. 2 Spatial distribution of annual NPP (**a**) and its CV (**c**) in NWC as well as boxplots of annual NPP (**b**) and its CV (**d**) for each province during the period from 2000 to 2015

Fig. 3 Change trend of average annual NPP in NWC from 2000 to 2015

$y=0.8443x-1608.16$
$R^2=0.73$ $p<0.05$

here showed a fluctuating upward trend ($p<0.05$) with an average increasing rate of 0.84 g C m^{-2} yr^{-1}. NPP was lower than the multi-year means in years 2000, 2001, 2002, 2008, and 2011.

The spatial distribution of NPP change rate is shown in Fig. 4a. In 88.2% of NWC, the change rate of NPP ranged from −10 to 10%. The small decreasing change rate of NPP, ranging from −10 to 0%, occurred in 18.8% of the study area, mainly distributed in northern Xinjiang. In 80.6% of the entire region (Fig. 4b), NPP showed increasing change rates. In northern Shaanxi, southern Ningxia, and eastern Gansu, the change rate of NPP was above 10% (Fig. 4a). At the provincial level, Ningxia had the highest change rate of NPP (7.7%), followed by Shaanxi (6.5%), Gansu (4.5%), Qinghai (3.8%), and Xinjiang (1.7%).

Mutation analysis of NPP in NWC

The Mann-Kendall test indicated that provincial mean NPP in Gansu, Ningxia, and Shaanxi showed a significant upward trend from 2000 to 2015 ($Z>1.96$). Meanwhile, the upward trend of NPP in Qinghai and Xinjiang was not significant ($Z<1.96$) (Fig. 5). The mutation test showed that NPP mutations occurred in all provinces. In Gansu, the NPP mutation occurred in 2007 with a decrease of 10 g C m^{-2} yr^{-1} in annual NPP, mainly caused by NPP reduction in central Gansu (Qilian mountains). In Ningxia, NPP changed abruptly in 2004 and 2009, respectively. Specifically, annual NPP decreased by 23.0 g C m^{-2} yr^{-1} in 2005 compared to that in 2004, while annual NPP was increasing year by year until 2004. Similarly, annual NPP decreased by 1.85 g C m^{-2} yr^{-1} in 2009 compared to that in 2008, while annual NPP increased substantially with a value of 22.45 g C m^{-2} yr^{-1} in

2010 compared to that in 2009. In Shaanxi, NPP showed mutations in 2004 and 2008. Annual NPP decreased by 27.7 and 3.1 g C m^{-2} yr^{-1} in the 2 years, respectively. As to Qinghai, NPP changed abruptly between 2002 and 2003. The provincial mean annual NPP decreased by 2.48 g C m^{-2} yr^{-1} in 2003 relative to the value in 2002. Xinjiang had the highest number of NPP mutations, which occurred in 2002, 2007, 2010, and 2014, respectively, in which NPP changed by 2.49, 1.72, 0.62, and −5.57 g C m^{-2} yr^{-1} in comparison to values in previous years.

Effects of water stress on NPP in NWC

The change rate of annual mean CWSI in NWC from 2000 to 2014 is shown in Fig. 6. CWSI decreased in areas of about 928262 km^2, accounting for 59.65% of the regional total. The increase in CWSI mainly occurred in the northern of Xinjiang, the southern of Qinghai, and Shaanxi. The decreasing rate of CWSI exceeded 30% in areas of about 882311 km^2. The areas, in which CWSI increased, amounted to about 627823 km^2 and were mainly distributed in the eastern of Qinghai, the southeastern of Gansu, the northern of Shaanxi, and the Kunlun Mountains in Xinjiang. The increasing rate of CWSI exceeded 30% in areas of about 587669 km^2. It means that the water stress condition in those regions had been increasing significantly. Overall, CWSI decreased and increased in 59.65% and 40.35% of the entire region, indicating that water stress decreased in most of the study area.

Figure 6b shows the correlation coefficient between NPP and CWSI in NWC. NPP was negatively correlated with CWSI in about 73.1 % of NWC (about 1125184 km^2), indicating that the NPP was restricted by water stress in most of NWC. In areas of about 468660 km^2 (30.4%), the negative
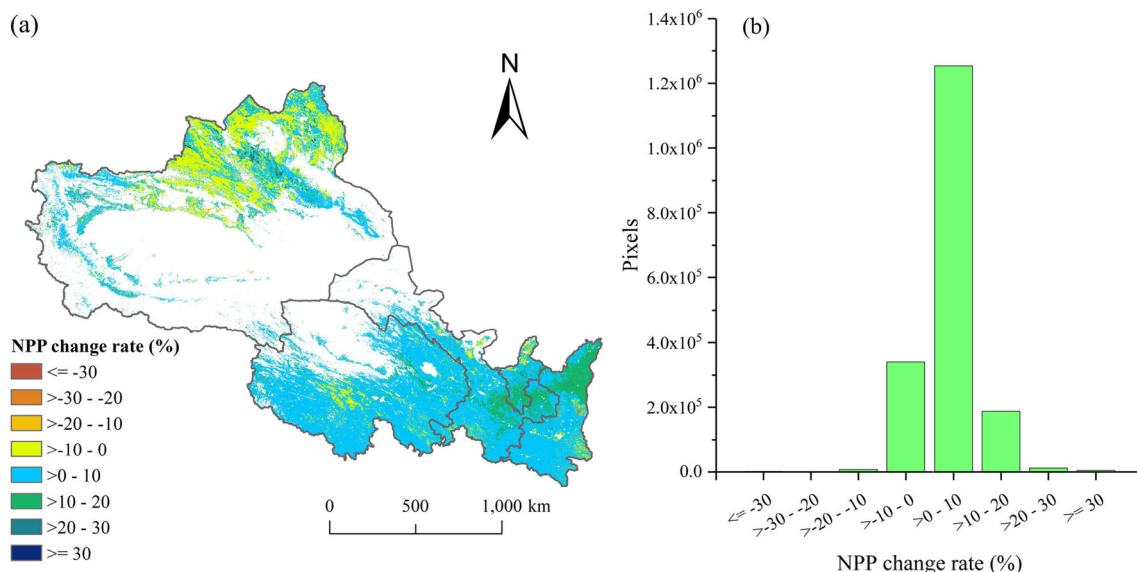

Fig. 4 Spatial distribution of NPP change rate (**a**) and number of pixels at each range of change rates (**b**) during the period from 2000 to 2015
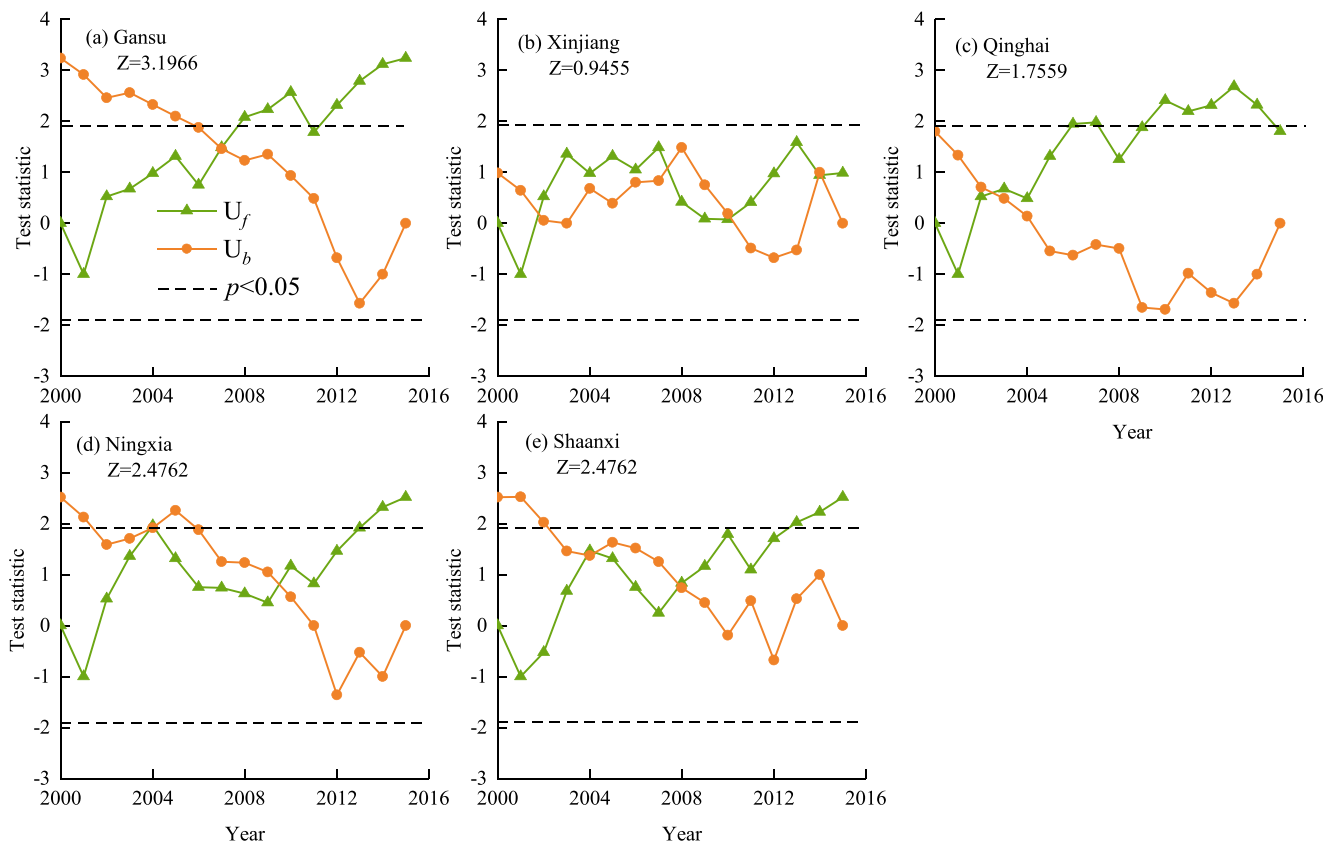
Fig. 5 Mann-Kendall trend and mutation test results of provincial mean NPP in NWC. a Gansu, b Xinjiang, c Qinghai, d Ningxia, e Shaanxi

correlation between NPP and CWSI was significant ($p<0.05$), mainly distributed in the northwestern of Xinjiang, the southern of Ningxia, and the middle of Gansu. In about 26.9% of the region (415156 km^2), NPP was positively correlated with CWSI. The positive correlation between NPP and CWSI was only significant ($p<0.05$) in 2.4% of the region (37096 km^2), mainly distributed in the southwestern of Qinghai.

Figure 7a shows the overall change of NPP with CWSI. With the increase in CWSI from 0.3 upwards, annual NPP

significantly declined. In areas with CWSI in the range from 0 to 0.3, annual NPP was very low. These areas are mainly located in high altitudes (above 3000 m), such as the edges of the Qaidam Basin and the foothills of the Kunlun and Tianshan Mountains. Although adequate snow and ice melting water makes high-altitude areas less water stressed (Tang et al. 2019), low temperature here resulted in very low NPP (Guo et al. 2020) and high inter-annual variability (CV) of NPP (Fig. 7b). CV values of NPP did not show a noticeable
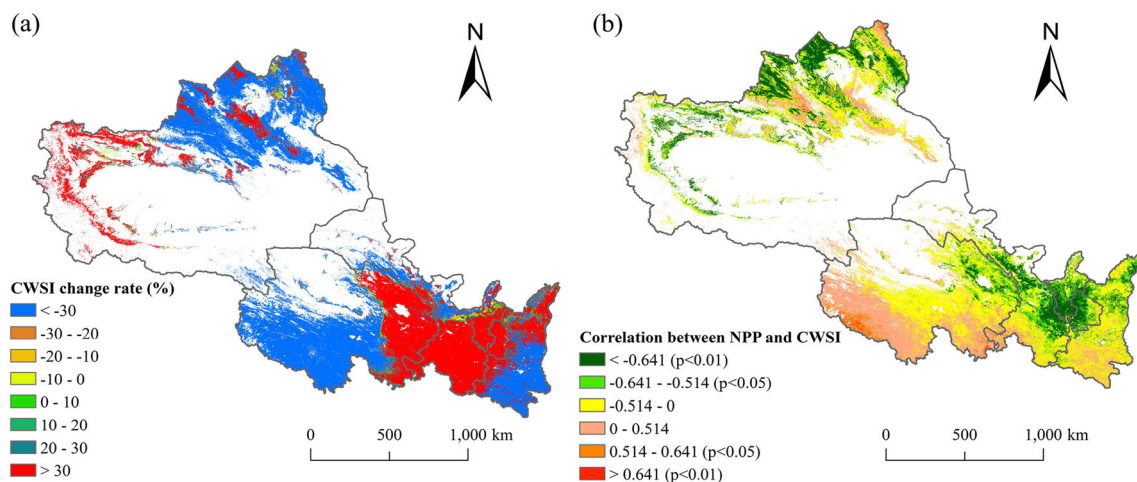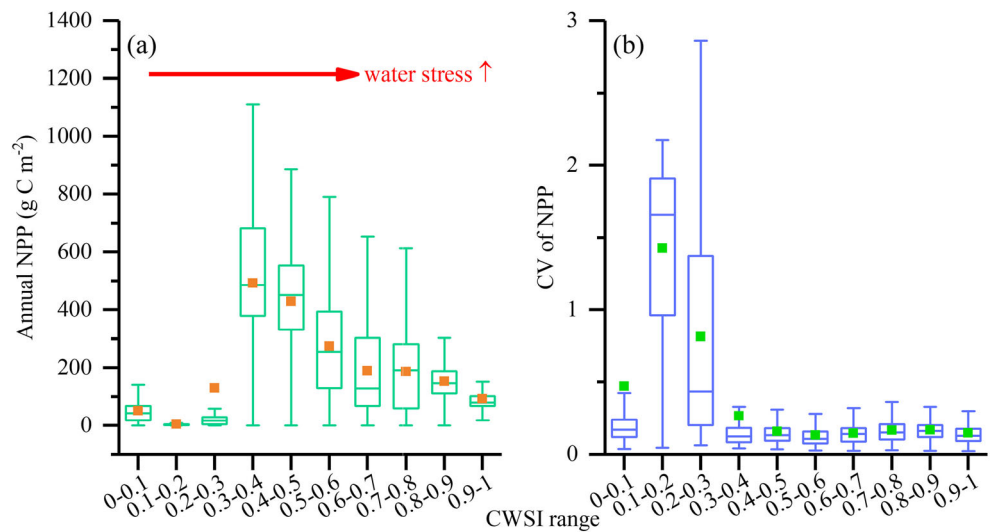

Fig. 6 Change rate of CWSI (a) and correlation between NPP and CWSI (b) in NWC

Fig. 7 Annual NPP (**a**) and its CV (**b**) under different CWSI intervals. The larger the CWSI is, the more severe the water stress is

changing pattern with CWSI under the conditions of CWSI above 0.3.

Discussion

Response of NPP to the change in water stress

In most of the region, annual NPP showed increasing trends and were negatively correlated with CWSI, indicating water stress acted as a key determinant of NPP trends and inter-annual variability in NWC. As shown in Fig. 8, with the decreasing change rate of CWSI (from positive to negative), the change rate of NPP starts to increase (from negative to positive). With 0 as the splitting point, the average rate of change of NPP was 8.91% when the rate of change of CWSI was less than 0, i.e., when water stress started to diminish. When the rate of change of CWSI was greater than 0, i.e., when water stress started to increase, the average rate of change of NPP

was only 0.01%. This significant difference further illustrates the significant limiting effect of water stress on NPP.

Previous studies reported larger reduction of NPP caused by water stress than this study (Wang et al. 2016a; Zhang et al. 2007a). This phenomenon can be explained by two reasons. On the one hand, plants in chronically water-deficient areas, such as NWC, are extremely efficient in water use, which makes them highly resistant to short-term droughts (Zhang et al. 2016). Thus, even if a small increase in water stress occurs, NPP would not significantly decrease. Of course, when water stress increases to very high levels, vegetation growth in these areas will still be affected (Liu et al. 2015; Lu and Zhuang 2010). In this study, when the change rate of CWSI increased above 60%, NPP showed apparent decreases (Fig. 8). On the other hand, artificial irrigation would sufficiently alleviate the negative impact of natural water stress on plants. Efficient water-saving irrigation, as one of the important measures to mitigate drought in water-deficient regions, has been widely implemented in agriculture in NWC (Chang

Fig. 8 Change rates of NPP in different ranges of CWSI change rates
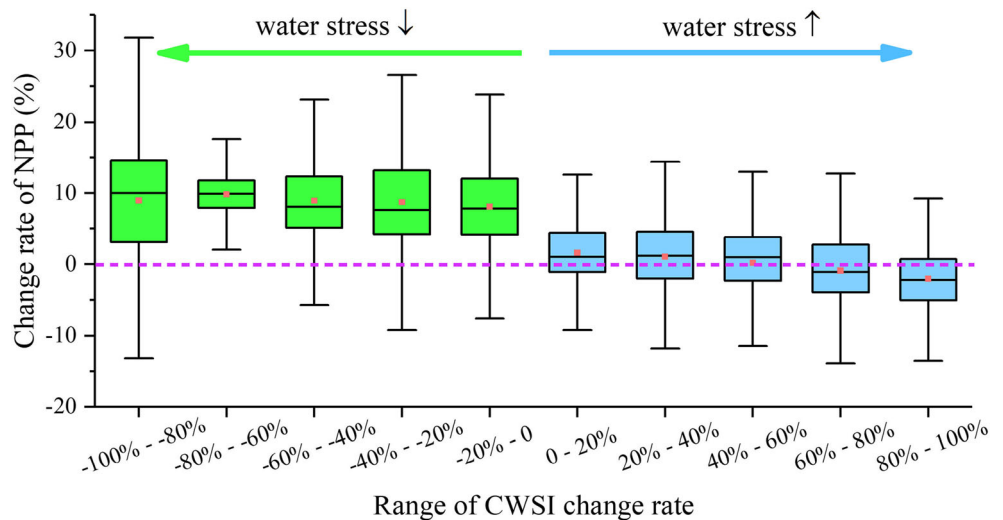
et al. 2016; Yang et al. 2020; Yue et al. 2016). This active manual intervention makes that even though CWSI is increasing, the actual water stress on the plant does not increase significantly (Belder et al. 2005; Ghrab et al. 2013; Zhu et al. 2014).

When the mean change rates of CWSI were less than 0, i.e., decrease in water stress, NPP increased apparently, with mean increase rates averaged 8.91%. This is consistent with the findings in many other regions, such as Sahel (Fensholt et al. 2006), Mongolia (Poulter et al. 2013), and Amazonia (Lee et al. 2013). However, the increase rate of NPP did not greatly increase with further decrease of CWSI. Areas with large magnitudes of CWSI normally have high elevations (Figs. 1 and 6). Temperature is also a key factor controlling vegetation growth and NPP here (Dai et al. 2011; Wang et al. 2020a). The positive effect of decrease in water stress on NPP might be offset by temperature since increase in precipitation is normally accomplished with decrease in temperature.

Change in the response of NPP to water stress with elevation

Hydrothermal conditions change with elevation. As a consequence, the growth of vegetation differs at different elevations (Huang et al. 2020; Sun et al. 2020a; Sun et al. 2020b; Teng et al. 2020). Changes of NPP with elevation have been reported in numerous studies (Liu et al. 2018; Vetaas et al. 2019; Ye et al. 2019). NWC has large elevation gradients (maximum above 8000 m), which could also influence the correlation between NPP and water stress. Thus, we further investigated the change in the response of NPP to water stress in different elevation ranges (Fig. 9). When the elevation exceeds 4000 m, correlation coefficients between NPP and CWSI were mostly positive, indicating that water stress was not a limiting factor of NPP. In NWC, the areas with elevation over 4000 m are mainly distributed in western Qinghai and the foothills of Kunlun Mountains. In these highly elevated areas, temperature also acts as the key determinant of NPP.

Under the condition of elevation below 4000 m, correlation coefficients between NPP and CWSI were mostly negative. This means that water stress limits NPP. In areas with elevation below 2000 m, the negative correlation between NPP and CWSI becomes intensified with the increase of elevation. Water stress has the strongest negative impact on NPP in areas with elevation in the range from 1000 to 2000 m (Fig. 9). With further increase in elevation above 2000 m, the negative impact of water stress on NPP becomes weaker and weaker, indicated by the shift of the correlation coefficient between NPP and CWSI from negative to positive.

In general, this finding confirms the important role of elevation in regulating water stress and affecting vegetation growth, which provides new ideas for studying the response of vegetation to environmental changes.
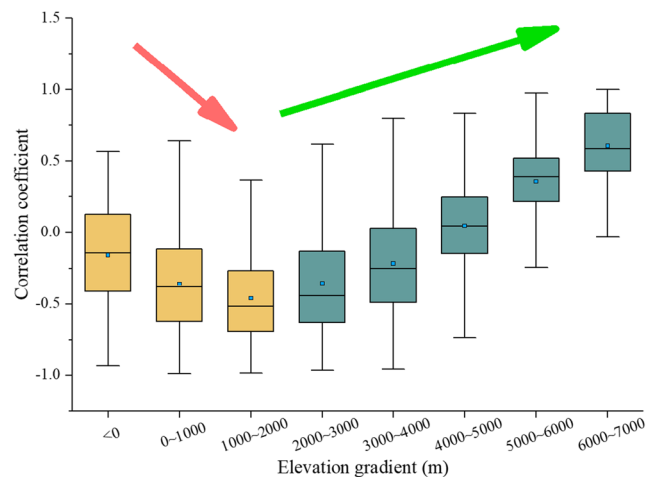

Fig. 9 Correlation between NPP and CWSI at different elevation gradients

Change in the relationship between NPP and water stress under various vegetation types

The difference in the characteristics of vegetation determines the response of various vegetation to the external environment is also different (Chen et al. 2020; Wu et al. 2015), for example, the response to water stress (Lian et al. 2021; Porporato et al. 2001). Thus, we further compared the relationship between NPP and water stress of various vegetation types in NWC (Fig. 10). On the whole, the vast majority of NPP and CWSI show a negative correlation, which once again shows that water stress is an important factor limiting NPP. At the same time, it is noted that there are also large differences in the correlation between NPP and water stress in various vegetations. Specifically, NPP in CRO was most closely related to water stress, with an average correlation of −0.45, followed by GRA (−0.24), DBF (−0.2), WS (−0.13), CNVM (−0.13), SAV (−0.04), and MF (−0.03). The strong correlation between farmland NPP and water stress indicates that the crop yield of NWC is still severely restricted by natural water conditions. Artificial water regulation techniques such as high-efficiency water-saving irrigation still have a lot of room for expansion in NWC (Du et al. 2014; Zou et al. 2020).

On the other hand, after comparing the two major forest types (DBF and MF), we found that MF was significantly less dependent on water stress than DBF, suggesting that MF may be better adapted to the drought environment of NWC and reminding us that mixed forest species may have greater environmental resistance due to higher biodiversity compared to single forest species (Ammer 2019; Jactel et al. 2017; Spiecker 2003). The results of three vegetation types dominated by herbaceous plants (GRA, SAV, and WS) show that NPP in pure grasslands (GRA) is the most sensitive to water stress, while vegetation NPP mixed with shrubs and other woody plants is much weaker in response to water stress.
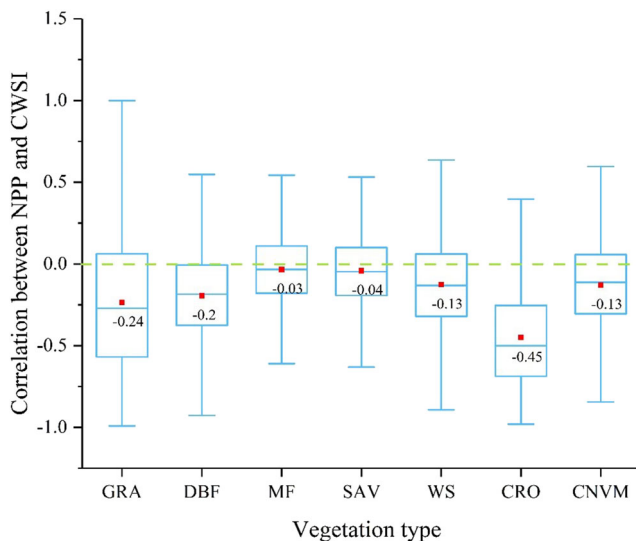
Fig. 10 Correlation between NPP and CWSI under various vegetation types in NWC. GRA, grasslands; DBF, deciduous broadleaf forests; MF, mixed forests; SAV, savannas; WS, woody savannas; CRO, croplands; CNVM, cropland or natural vegetation mosaics

Fig. 11 The consistency in past and future trends of NPP over NWC

Overall, NPP in single vegetation type showed a stronger relationship to water stress, while the NPP in mixed vegetation types showed a lower dependence to water stress. This finding inspires us that forest and grass symbiosis may be a feasible path for ecologically sustainable development in NWC, rather than a single tree planting afforestation (Brancalion and Holl 2020; Grossnickle and Ivetić 2017; Steidinger et al. 2019).

Consistency in past and future trends of NPP

The consistency in past and future trends of NPP was analyzed according to the Hurst index (Fig. 11). Values in Fig. 11 were determined on the basis of Hurst index and trends of NPP during the period from 2000 to 2015. In 58% of the region, past and future trends of NPP are inconsistent ($H<0.5$). In 11% of the entire region, NPP showed a decreasing trend during the period from 2000 to 2015 and might increase in the future, mainly located in the northern of Xinjiang. In 47% of the region, NPP increased in the past and might decrease in the future, mainly located in the eastern of Qinghai. In 34% of the entire region, NPP might keep the increase trend in the future, mainly located in Shaanxi, the southern of Gansu, and the western of Qinghai. Overall, future increase and decrease in NPP might occur in 46% and 54% of the region, respectively.

It should be kept in mind that the future trend of NPP projected by the Hurst index does not consider the effects of human activities on NPP. In practice, some human activities could offset negative impacts of natural conditions on NPP to some extent. Hao et al. (2020) found that straw returning and fertilization could significantly increase the accumulation of organic carbon and productivity in farmlands over NWC. Li et al. (2012) pointed out that high-efficiency water-saving
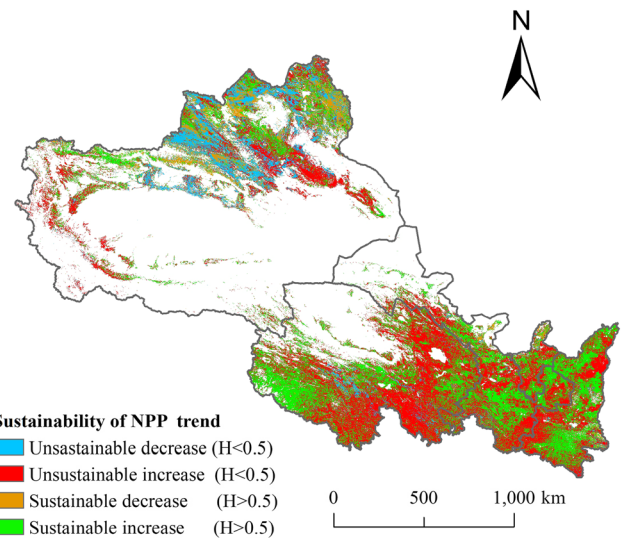
irrigation significantly increased the productivity and yield of crops in this region. Niu et al. (2019) declared that the vegetation coverage and aboveground biomass could be significantly enhanced here by proper ecological engineering. Thus, the shift of NPP from increase to decrease in some areas could be alleviated or reversed through positive human activities.

Conclusion

In this study, MODIS NPP and ET products were used to analyze the dynamics of NPP and its response to water stress indicated by CWSI in NWC. The main findings are the following:

(1) NPP increased in 80.6% of NWC during the period from 2000 to 2015. The increasing rate averaged 0.84 g C m^{-2} yr^{-1}. At the provincial level, Gansu had the most increase of NPP, followed by Shaanxi, Ningxia, Qinghai, and Xinjiang.

(2) Water stress acted as controlling factor of NPP in most of NWC. In about 73.1% of this region, annual NPP was negatively correlated with annual mean CWSI. Overall, NPP decreased with the increase of CWSI under the condition of CWSI above 0.3, accounting for the 45.28% of the entire region.

(3) NPP in CRO was most closely related to CWSI, with an average correlation coefficient of −0.45, followed by GRA (−0.24), DBF (−0.2), WS (−0.13), CNVM (−0.13), SAV (−0.04), and MF (−0.03). NPP in single vegetation type showed a stronger relationship to water stress, while the NPP in mixed vegetation types showed a lower dependence to water stress.

(4) The response of NPP to water stress varies with elevation. The negative impact of water stress on NPP was the strongest at elevations about 2000 m. With further increase of elevation above 2000 m, the control of water stress on NPP became weaker and weaker. At elevations above 5000 m, the correlation between NPP and WSI was mostly positive.

Our results highlighted the limiting effect of water stress on NPP in arid region. This effect is elevation dependent, which is important for better projection of the response of vegetation to climate change. Of course, there are some uncertainties in this study, mainly caused by uncertainties of NPP, ET, and PET data used, the exclusion of deserts and semi-deserts, and relatively short study period. These issues need be well investigated in the future.

Availability of data and materials All data generated or analyzed during this study are included in this article.

Declarations

Ethics approval The manuscript does not report on or involve the use of any animal or human data.

Consent to participate Nobody participated in the human or animal experiment.

Consent for publication All authors agreed to publish the article.

Competing interests The authors declare no competing interests.

References

Alharbi S, Raun WR, Arnall DB, Zhang H (2019) Prediction of maize (Zea mays L.) population using normalized-difference vegetative index (NDVI) and coefficient of variation (CV). J. Plant Nutr 42: 673–679

Ammer C (2019) Diversity and forest productivity in a changing climate. New Phytol 221:50–66

Azhdari Z, Sardooi ER, Bazrafshan O, Zamani H, Singh VP, Saravi MM, Ramezani M (2020) Impact of climate change on net primary production (NPP) in south Iran. Environ Monit Assess 192:409

Bastos A, Running SW, Gouveia C, Trigo RM (2013) The global NPP dependence on ENSO: La Nina and the extraordinary year of 2011. Journal of Geophysical Research-Biogeosciences 118:1247–1255

Belder P, Spiertz JHJ, Bouman BAM, Lu G, Tuong TP (2005) Nitrogen economy and water productivity of lowland rice under water-saving irrigation. Field Crop Res 93:169–185

Berni JAJ, Zarco-Tejada PJ, Sepulcre-Canto G, Fereres E, Villalobos F (2009) Mapping canopy conductance and CWSI in olive orchards using high resolution thermal remote sensing imagery. Remote Sens Environ 113:2380–2388

Brancalion PHS, Holl KD (2020) Guidance for successful tree planting initiatives. J Appl Ecol 57:2349–2361

Burn DH, Elnur MAH (2002) Detection of hydrologic trends and variability. J Hydrodyn 255:107–122

Chang G, Wang L, Meng L, Zhang W (2016) Farmers' attitudes toward mandatory water-saving policies: a case study in two basins in northwest China. J Environ Manag 181:455–464

Chen Z, Wang W, Fu J (2020) Vegetation response to precipitation anomalies under different climatic and biogeographical conditions in China. Sci Rep 10:1–16

Ciais P, Reichstein M, Viovy N, Granier A, Ogée J, Allard V, Aubinet M, Buchmann N, Bernhofer C, Carrara A, Chevallier F, de Noblet N, Friend AD, Friedlingstein P, Grünwald T, Heinesch B, Keronen P, Knohl A, Krinner G, Loustau D, Manca G, Matteucci G, Miglietta F, Ourcival JM, Papale D, Pilegaard K, Rambal S, Seufert G, Soussana JF, Sanz MJ, Schulze ED, Vesala T, Valentini R (2005) Europe-wide reduction in primary productivity caused by the heat and drought in 2003. Nature 437:529–533

Cox GJ, Matuschak MC (1941) An abbreviation of the method of least squares. JPhCh 45:362–369

Cramer W, Field CB (1999) Comparing global models of terrestrial net primary productivity (NPP): introduction. Glob Chang Biol 5:56–64

Dai S, Zhang B, Wang H, Wang Y, Guo L, Wang X, Li D (2011) Vegetation cover change and the driving factors over northwest China. Journal of Arid Land 3:25–33

Drechsler K, Kisekka I, Upadhyaya S (2019) A comprehensive stress indicator for evaluating plant water status in almond trees. Agric Water Manag 216:214–223

Du T, Kang S, Zhang X, Zhang J (2014) China's food security is threatened by the unsustainable use of water resources in North and Northwest China. Food and Energy Security 3:7–18

Euskirchen ES, Chen JQ, Li HB, Gustafson EJ, Crow TR (2002) Modeling landscape net ecosystem productivity (LandNEP) under alternative management regimes. Ecol Model 154:75–91

Ezenne GI, Jupp L, Mantel SK, Tanner JL (2019) Current and potential capabilities of UAS for crop water productivity in precision agriculture. Agric Water Manag 218:158–164

Feng X, Liu G, Chen JM, Chen M, Liu J, Ju WM, Sun R, Zhou W (2007) Net primary productivity of China's terrestrial ecosystems from a process model driven by remote sensing. J Environ Manag 85:563–573

Fensholt R, Sandholt I, Rasmussen MS, Stisen S, Diouf A (2006) Evaluation of satellite based primary production modelling in the semi-arid Sahel. Remote Sens Environ 105:173–188

Gerhards M, Rock G, Schlerf M, Udelhoven T (2016) Water stress detection in potato plants using leaf temperature, emissivity, and reflectance. IJAEO 53:27–39

Ghrab M, Zitouna R, Ben Mimoun M, Masmoudi MM, Ben Mechlia N (2013) Yield and water productivity of peach trees under continuous deficit irrigation and high evaporative demand. Biol Agric Hortic 29:29–37

Gong SQ, Hagan DFT, Wu XY, Wang GJ (2018) Spatio-temporal analysis of precipitable water vapour over northwest china utilizing MERSI/FY-3A products. Int J Remote Sens 39:3094–3110

Grossnickle SC, Ivetić V (2017) Direct seeding in reforestation–a field performance review. Reforesta 4:94–142

Guo B, Zang W, Yang F, Han B, Chen S, Liu Y, Yang X, He T, Chen X, Liu C, Gong R (2020) Spatial and temporal change patterns of net primary productivity and its response to climate change in the Qinghai-Tibet Plateau of China from 2000 to 2015. Journal of Arid Land 12:1–17

Hao X, He W, Lam SK, Li P, Zong Y, Zhang D, Li FY (2020) Enhancement of no-tillage, crop straw return and manure application on field organic matter content overweigh the adverse effects of climate change in the arid and semi-arid Northwest China. Agric For Meteorol 295:1–10

Hasenauer H, Petritsch R, Zhao M, Boisvenue C, Running SW (2012) Reconciling satellite with ground data to estimate forest productivity at national scales. For Ecol Manag 276:196–208

Hein A, Condon L, Maxwell R (2019) Evaluating the relative importance of precipitation, temperature and land-cover change in the hydrologic response to extreme meteorological drought conditions over the North American High Plains. HESS 23:1931–1950

Hsiao TC (1973) Plant responses to water stress. Annu Rev Plant Physiol Plant Mol Biol 24:519–570

Huang X, Huang C, Teng M, Zhou Z, Wang P (2020) Net primary productivity of Pinus massoniana dependence on climate, soil and forest characteristics. Forests 11:404

Hurst HE (1951) Long-term storage capacity of reservoirs. Trans Am Soc Civ Eng 116:770–799

Irmak S, Haman DZ, Bastug R (2000) Determination of crop water stress index for irrigation timing and yield estimation of corn. Agron J 92:1221–1227

Jackson RD (1982) Soil-moisture inferences from thermal-infrared measurements of vegetation temperatures. ITGRS 20:282–286

Jackson RD, Idso SB, Reginato RJ, Pinter PJ (1981) Canopy temperature as a crop water-stress indicator. WRR 17:1133–1138

Jactel H, Bauhus J, Boberg J, Bonal D, Castagneyrol B, Gardiner B, Gonzalez-Olabarria JR, Koricheva J, Meurisse N, Brockerhoff EG (2017) Tree diversity drives forest stand resistance to natural disturbances. Current Forestry Reports 3:223–243

Jia L, Z-b L, Xu G-c, Z-p R, Li P, Cheng Y-t, Y-x Z, Wang B, Zhang J-x YS (2020) Dynamic change of vegetation and its response to climate and topographic factors in the Xijiang River basin, China. Environ Sci Pollut Res 27:11637–11648

Jiang L, Jiapaer G, Bao A, Guo H, Ndayisaba F (2017) Vegetation dynamics and responses to climate change and human activities in Central Asia. Sci Total Environ 599:967–980

Kullberg EG, DeJonge KC, Chavez JL (2017) Evaluation of thermal remote sensing indices to estimate crop evapotranspiration coefficients. Agric Water Manag 179:64–73

Lee J-E, Frankenberg C, van der Tol C, Berry JA, Guanter L, Boyce CK, Fisher JB, Morrow E, Worden JR, Asefi S, Badgley G, Saatchi S (2013) Forest productivity and water stress in Amazonia: observations from GOSAT chlorophyll fluorescence. Proceedings of the Royal Society B-Biological Sciences 280:176–188

Li Z, Pan J (2018) Spatiotemporal changes in vegetation net primary productivity in the arid region of Northwest China, 2001 to 2012. Front Earth Sci 12:108–124

Li ZG, Zhang RH, Wang XJ, Chen F, Tian CY (2012) Growing season carbon dioxide exchange in flooded non-mulching and non-flooded mulching cotton. PLoS ONE 7(11): e50760

Li X, Farooqi TJA, Jiang C, Liu S, Sun OJ (2019) Spatiotemporal variations in productivity and water use efficiency across a temperate forest landscape of Northeast China. For Ecosyst 6:22

Li D, Xu E, Zhang H (2020) Influence of ecological land change on wind erosion prevention service in arid area of northwest China from 1990 to 2015. Ecol Indic 117:106686

Li H, Zhang HY, Li QX, Zhao JJ, Guo XY, Ying H, Deng GR, Wu RH, Wang SL (2021) vegetation productivity dynamics in response to climate change and human activities under different topography and land cover in Northeast China. Remote Sens 13(5):975

Lian X, Piao S, Chen A, Huntingford C, Fu B, Li LZX, Huang J, Sheffield J, Berg AM, Keenan TF (2021) Multifaceted characteristics of dryland aridity changes in a warming world. Nat Rev Ear Envir 2:232–250

Liu H, Weng Q (2018) Scaling effect of fused ASTER-MODIS land surface temperature in an urban environment. Sensors (Basel) 18:4058

Liu Y, Xiao J, Ju W, Zhou Y, Wang S, Wu X (2015) Water use efficiency of China's terrestrial ecosystems and responses to drought. Sci Rep 5:13799

Liu SL, Cheng FY, Dong SK, Zhao HD, Hou XY, Wu X (2017): Spatiotemporal dynamics of grassland aboveground biomass on the Qinghai-Tibet Plateau based on validated MODIS NDVI. Sci Rep 7:4182

Liu H, Mi Z, Lin L, Wang Y, Zhang Z, Zhang F, Wang H, Liu L, Zhu B, Cao G, Zhao X, Sanders NJ, Classen AT, Reich PB, He J-S (2018) Shifting plant species composition in response to climate change stabilizes grassland primary production. Proc Natl Acad Sci U S A 115:4051–4056

Liu P, Song H, Wang T, Wang F, Li X, Miao C, Zhao H (2020) Effects of meteorological conditions and anthropogenic precursors on ground-level ozone concentrations in Chinese cities. Environ Pollut 262:114366

Lou W, Sun S, Sun K, Yang X, Li S (2017) Summer drought index using SPEI based on 10-day temperature and precipitation data and its application in Zhejiang Province (Southeast China). Stoch Env Res Risk A 31:2499–2512

Lu X, Zhuang Q (2010) Evaluating evapotranspiration and water-use efficiency of terrestrial ecosystems in the conterminous United States using MODIS and AmeriFlux data. Remote Sens Environ 114:1924–1939

Monteith JL (1965) Evaporation and environment. Symp Soc Exp Biol 19:205–234

Monteith JL (1981) Evaporation and surface-temperature. QJRMS 107:1–27

Mu Q, Zhao M, Running SW (2011) Improvements to a MODIS global terrestrial evapotranspiration algorithm. Remote Sens Environ 115:1781–1800

Munns R (2002) Comparative physiology of salt and water stress. Plant Cell Environ 25:239–250

Na SI, Ahn HY, Park CW, Hong SY, So KH, Lee KD (2020) Crop water stress index (CWSI) mapping for evaluation of abnormal growth of spring Chinese cabbage using drone-based thermal infrared image. Korean Journal of Remote Sensing 36:667–677

Nagler PL, Scott RL, Westenburg C, Cleverly JR, Glenn EP, Huete AR (2005) Evapotranspiration on western US rivers estimated using the enhanced vegetation index from MODIS and data from eddy covariance and Bowen ratio flux towers. Remote Sens Environ 97:337–351

Nemani RR, Keeling CD, Hashimoto H, Jolly WM, Piper SC, Tucker CJ, Myneni RB, Running SW (2003) Climate-driven increases in global terrestrial net primary production from 1982 to 1999. Sci 300:1560–1563

Niu Q, Xiao X, Zhang Y, Qin Y, Dang X, Wang J, Zou Z, Doughty RB, Brandt M, Tong X, Horion S, Fensholt R, Chen C, Myneni RB, Xu W, Di G, Zhou X (2019) Ecological engineering projects increased vegetation cover, production, and biomass in semiarid and subhumid Northern China. LDD 30:1620–1631

Pan J, Dong L (2018) Spatio-temporal variation in vegetation net primary productivity and its relationship with climatic factors in the Shule River basin from 2001 to 2010. Hum Ecol Risk Assess 24:797–818

Pan YX, Wang XP, Ma XZ, Zhang YF, Hu R (2020) The stable isotopic composition variation characteristics of desert plants and water sources in an artificial revegetation ecosystem in Northwest China. Catena 189:104499

Penuelas J et al (2007) Response of plant species richness and primary productivity in shrublands along a north-south gradient in Europe to seven years of experimental warming and drought: reductions in primary productivity in the heat and drought year of 2003. Glob Chang Biol 13:2563–2581

Pettitt AN (1979) A non-parametric approach to the change-point problem. J Roy Stat Soc Ser C (Appl Stat) 28:126–135

Porporato A, Laio F, Ridolfi L, Rodriguez-Iturbe I (2001) Plants in water-controlled ecosystems: active role in hydrologic processes and response to water stress: III. Vegetation water stress AdWR 24:725–744

Pou A, Diago MP, Medrano H, Baluja J, Tardaguila J (2014) Validation of thermal indices for water status identification in grapevine. Agric Water Manag 134:60–72

Poulter B, Pederson N, Liu H, Zhu Z, D'Arrigo R, Ciais P, Davi N, Frank D, Leland C, Myneni R, Piao S, Wang T (2013) Recent trends in Inner Asian forest dynamics to temperature and precipitation indicate high sensitivity to climate change. Agric For Meteorol 178:31–45

Qu S, Wang L, Lin A, Yu D, Yuan M, Ca L (2020) Distinguishing the impacts of climate change and anthropogenic factors on vegetation dynamics in the Yangtze River Basin, China. Ecol Indic 108:105724

Rahman MA, Lou Y, Sultana N (2017) Analysis and prediction of rainfall trends over Bangladesh using Mann-Kendall, Spearman's rho tests and ARIMA model. MAP 129:409–424

Rojo Baio FH, Neves DC, Teodoro PE (2019) Soil chemical attributes, soil type, and rainfall effects on normalized difference vegetation index and cotton fiber yield variability. Agron J 111:2910–2919

Running SW, Nemani RR, Heinsch FA, Zhao MS, Reeves M, Hashimoto H (2004) A continuous satellite-derived measure of global terrestrial primary production. Bioscience 54:547–560

Saigusa N, Yamamoto S, Hirata R, Ohtani Y, Ide R, Asanuma J, Gamo M, Hirano T, Kondo H, Kosugi Y, Li S-G, Nakai Y, Takagi K, Tani M, Wang H (2008) Temporal and spatial variations in the seasonal patterns of CO$_2$ flux in boreal, temperate, and tropical forests in East Asia. Agric For Meteorol 148:700–713

Spiecker H (2003) Silvicultural management in maintaining biodiversity and resistance of forests in Europe—temperate zone. J Environ Manag 67:55–65

Steidinger BS, Crowther TW, Liang J, Van Nuland ME, Werner GDA, Reich PB, Nabuurs G-J, De-Miguel S, Zhou M, Picard N (2019) Climatic controls of decomposition drive the global biogeography of forest-tree symbioses. Nature 569:404–408

Street GM, McNickle GG (2019) A global estimate of terrestrial net secondary production of primary consumers. Glob Ecol Biogeogr 28:1763–1773

Sun J, Wen Z, Feijo A, Cheng J, Wang Y, Li S, Ge D, Xia L, Yang Q (2020a) Elevation patterns and critical environmental drivers of the taxonomic, functional, and phylogenetic diversity of small mammals in a karst mountain area. Ecology and Evolution 10:10899–10911

Sun X, Wang G, Huang M, Chang R, Hu Z, Song C, Sun J (2020b) The asynchronous response of carbon gain and water loss generate spatio-temporal pattern of WUE along elevation gradient in southwest China. JHyd 581:124389

Tang Q, Lan C, Su F, Liu X, Sun H, Ding J, Wang L, Leng G, Zhang Y, Sang Y, Fang H, Zhang S, Han D, Liu X, He L, Xu X, Tang Y, Chen D (2019) Streamflow change on the Qinghai-Tibet Plateau and its impacts. Chinese Science Bulletin-Chinese 64:2807–2821

Tatarinov F, Rotenberg E, Maseyk K, Ogee J, Klein T, Yakir D (2016) Resilience to seasonal heat wave episodes in a Mediterranean pine forest. New Phytol 210:485–496

Teng M, Zeng L, Hu W, Wang P, Yan Z, He W, Zhang Y, Huang Z, Xiao W (2020) The impacts of climate changes and human activities on net primary productivity vary across an ecotone zone in Northwest China. Sci Total Environ 714:136691

Tong S, Lai Q, Zhang J, Bao Y, Lusi A, Ma Q, Li X, Zhang F (2018) Spatiotemporal drought variability on the Mongolian Plateau from 1980-2014 based on the SPEI-PM, intensity analysis and Hurst exponent. Sci Total Environ 615:1557–1565

Turner DP, Ritts WD, Cohen WB, Gower ST, Running SW, Zhao MS, Costa MH, Kirschbaum AA, Ham JM, Saleska SR, Ahl DE (2006) Evaluation of MODIS NPP and GPP products across multiple biomes. Remote Sens Environ 102:282–292

Velpuri NM, Senay GB, Singh RK, Bohms S, Verdin JP (2013) A comprehensive evaluation of two MODIS evapotranspiration products over the conterminous United States: using point and gridded FLUXNET and water balance ET. Remote Sens Environ 139:35–49

Vetaas OR, Paudel KP, Christensen M (2019) Principal factors controlling biodiversity along an elevation gradient: water, energy and their interaction. J Biogeogr 46:1652–1663

Wang W, Wang J, Liu X, Zhou G, Yan J (2016a) Decadal drought deaccelerated the increasing trend of annual net primary production in tropical or subtropical forests in southern China. Sci Rep 6:28640

Wang Z, Zhang Y, Yang Y, Zhou W, Gang C, Zhang Y, Li J, An R, Wang K, Odeh I, Qi J (2016b) Quantitative assess the driving forces on the grassland degradation in the Qinghai–Tibet Plateau, in China. Ecol Inform 33:32–44

Wang MJ, Liu G, Sun R, Xiao ZQ, Ieee (2019) Assessment of NPP dynamics and the responses to climate changes in china from 1982 to 2012, 2019 Ieee International Geoscience and Remote Sensing Symposium. IEEE International Symposium on Geoscience and Remote Sensing IGARSS. pp 6602–6605

Wang B, Xu G, Li P, Li Z, Zhang Y, Cheng Y, Jia L, Zhang J (2020a) Vegetation dynamics and their relationships with climatic factors in the Qinling Mountains of China. Ecol Indic 108:105719

Wang Y, Yue H, Peng Q, He C, Hong S, Bryan BA (2020b) Recent responses of grassland net primary productivity to climatic and anthropogenic factors in Kyrgyzstan. LDD 31:2490–2506

Wu D, Zhao X, Liang S, Zhou T, Huang K, Tang B, Zhao W (2015) Time-lag effects of global vegetation responses to climate change. Glob Chang Biol 21:3520–3531

Wu L, Wang S, Bai X, Luo W, Tian Y, Zeng C, Luo G, He S (2017) Quantitative assessment of the impacts of climate change and human activities on runoff change in a typical karst watershed. SW China Sci Total Environ 601:1449–1465

Xing Z, Yang Z, Fu Q, Li H, Gong X, Wu J (2017) Characteristics and risk assessment of agricultural meteorological disasters based on 30 years' disaster data from Heilongjiang Province of China. Int J Agric Biol Eng 10:144–154

Xue Y, Pan W, Lu W-Z, He H-D (2015) Multifractal nature of particulate matters (PMs) in Hong Kong urban air. Sci Total Environ 532:744–751

Yang G, Tian L, Li X, He X, Gao Y, Li F, Xue L, Li P (2020) Numerical assessment of the effect of water-saving irrigation on the water cycle at the Manas River Basin oasis. China Sci Total Environ 707: 135587

Yao Y, Sun J, Tian Y, Zheng C, Liu J (2020) Alleviating water scarcity and poverty in drylands through telecouplings: vegetable trade and tourism in northwest China. Sci Total Environ 741:140387–140387

Ye X-c, Y-k M, Xu L-g, Xu C-y (2019) Net primary productivity dynamics and associated hydrological driving factors in the floodplain wetland of China's largest freshwater lake. Sci Total Environ 659: 302–313

Yuan W, Liu S, Yu G, Bonnefond J-M, Chen J, Davis K, Desai AR, Goldstein AH, Gianelle D, Rossi F, Suyker AE, Verma SB (2010) Global estimates of evapotranspiration and gross primary production based on MODIS and global meteorology data. Remote Sens Environ 114:1416–1431

Yue W, Liu X, Wang T, Chen X (2016) Impacts of water saving on groundwater balance in a large-scale arid irrigation district, Northwest China. Irrig Sci 34:297–312

Zhang K, Kimball JS, McDonald KC, Cassano JJ, Running SW (2007a) Impacts of large-scale oscillations on pan-Arctic terrestrial net primary production. Geophys Res Lett 34:L21403

Zhang P, Fan Y, Luo W, Liu H, Wu W (2007b) Analysing the impact of meteorologic factors on NDVI. Progress of Information Technology in Agriculture 744-749

Zhang T, Peng J, Liang W, Yang Y, Liu Y (2016) Spatial-temporal patterns of water use efficiency and climate controls in China's loess plateau during 2000-2010. Sci Total Environ 565:105–122

Zhang T, Yu G, Chen Z, Hu Z, Jiao C, Yang M, Fu Z, Zhang W, Han L, Fan M, Zhang R, Sun Z, Gao Y, Li W (2020a) Patterns and controls of vegetation productivity and precipitation-use efficiency across Eurasian grasslands. Sci Total Environ 741:140204–140204

Zhang ZY, Li XY, Liu LJ, Wang YG, Li Y (2020b) Influence of mulched drip irrigation on landscape scale evapotranspiration from farmland in an arid area. Agric Water Manage 230:105953

Zhao MS, Heinsch FA, Nemani RR, Running SW (2005) Improvements of the MODIS terrestrial gross and net primary production global data set. Remote Sens Environ 95:164–176

Zhu C-G, Chen Y-N, Li W-H, Yang Y-H (2014) Photosynthetic performance of two poplar species in shelterbelt under water-saving irrigation in arid northwest China. Nord J Bot 32:602–610

Zou M, Kang S, Niu J, Lu H (2020) Untangling the effects of future climate change and human activity on evapotranspiration in the Heihe agricultural region, Northwest China. JHyd 585:124323

Publisher's note Springer Nature remains neutral with regard to jurisdictional claims in published maps and institutional affiliations.